THE IMPACT DAMAGE AND THE LOW COMPRESSIVE STRENGTH OF COMPOSITE LAMINATES

H. Suemasu
Department of Engineering and applied sciences, Sophia University, Tokyo, Japan
(suemasu@sophia.ac.jp)

Keywords: ***Laminate, Impact damage, Buckling, Finite element analysis, Energy release rate***

1. Introduction

Composite laminates are used particularly for aerospace structures due to their high specific strength and stiffness. It is necessary to evaluate the over-all performance of the composite laminates considering various damage tolerant properties based on the conditions of practical applications by appropriate methods. Compression after impact (CAI) test provides a design data for a compressive strength. Many researchers have studied CAI problem, since it is often critical in the design of aeronautical structures. However, the mechanical meaning of CAI strength is not very clear yet.

In the present paper meaning of CAI strength is discussed through experiment and analysis.

2. Experiment

Quasi-isotropic CFRP laminates $[(45/0/-45/90)_4]_{sym}$ was tested following SACMA standard of CAI. The material properties are listed in Table 1. Impact damage was introduced by using a drop weight test (32 J for IM600/#133 and 16 J for the T700/#2500). The impact damages could be said to take a double spiral shape and their diameters were 30-40 mm for both specimens. Compressive tests of the damaged specimens were done in a screw-driven test machine.

3. Finite Element Analysis

Compressive behavior of the Quasi-isotropic laminates with a spiral shape damage was numerically analyzed by a finite element method (Abaqus 6.7). Fig.1 shows an analytical model of a rectangular laminate with the damage consisting of inter-connecting delaminations of 1/8 sectors of a annular ring and transverse matrix cracks. Quadratic 20 node solid elements were used. The contact of the damaged portion was approximately considered by using a nonlinear spring elements. Material properties of IM600/#133 were used. Energy release rate along the delamination edges is calculated by VCCT. Several cases of different outside diameters d_o were analyzed. The diameter d_i of the center undamaged portion was set 5.0 mm.

4. Results And Discussions

The applied load was plotted against the cross-head displacement in Fig.2. Slight reduction of the stiffness occurred at about 80 kN for T700/#2500 and 100 kN for IM600/#133. The specimens failed at 102 kN and 116 kN, respectively. The C-scan images of the damage area was shown in Fig.3. For a IM600/#133 specimen, audible sound occurred several times without visible change of the damage in the C-scan images. Damage growth was found at the both sides of the damage just after a large sound at 119 kN at the fourth ply interface from the back surface. The specimen broke soon after the reloading. The final failure behavior of T700/#2500 specimen recorded by a high-speed video camera (Fig.4) showed unstable growth of the damage in transverse direction to the load. IM600/#133 specimen (not shown here) tended to break more violently at higher load than the T700/#2500 specimen.

Deflections of several points obtained by a finite element method are plotted against the load for the model of d_o=30 mm in Fig.5. The postbuckling was found to consist of four stages as

(a) Buckling of the surface delaminated portion
(b) Through-thickness local buckling
(c) Global symmetric plate buckling
(d) Global antisymmetric plate buckling

Stages (c) and (d) did not realize in the experiment owing to the specimen failure.

Energy release rate, calculated along the whole inside and outside edges of the spiral shape damage, had local maximum in the direction transverse to the load for outside edges and in the longitudinal direction for the inside edges. The maximum values of the energy release rate at the transverse edge for the cases d_o=30 mm and 40 mm are plotted in Fig. 6 with the test data (CAI strength vs. the Mode II interlaminar toughness). The test results well agrees with the possible strength supposed from the applied load and maximum energy release rate curves.

The author acknowledges M. Ichiki for his conducting finite element analyses, Dr. Aoki for his help to carry out CAI experiments and Dr. Ishikawa (JAXA) for the valuable advises and support during the collaborative research.

Table 1 Material properties of CFRP lamina

	E_L (GPa)	E_T (GPa)	G_{LT} (GPa)	ν_{LT}	G_{IC} (kJ/m^2)	G_{IIC} (kJ/m^2)
IM600/#133	152	8.2	4.4	0.33	0.44	1.86
T700/#2500	130	8.0	4.8	0.31	0.17	0.55

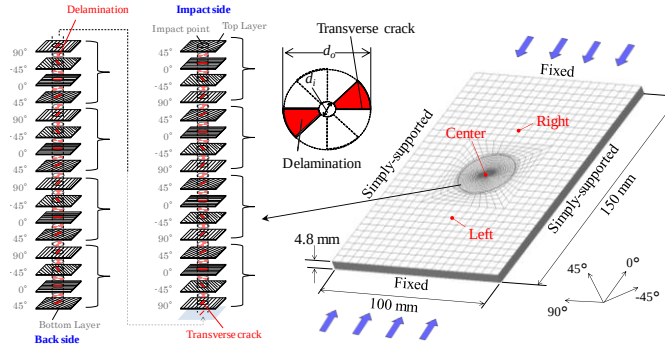

Fig.1 Spiral shape damage and finite element discretization.

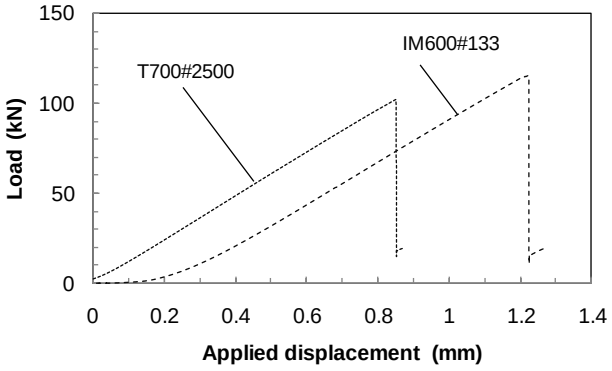

Fig.2 Relationships between the applied load and the cross-head displacement.

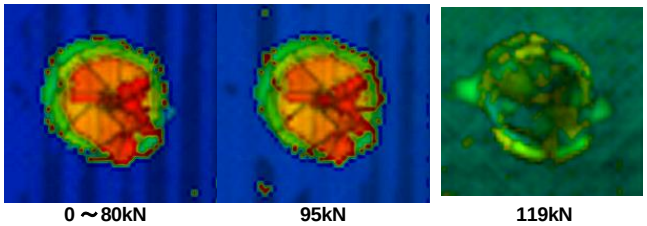

Fig. 3 The ultrasonic images of the impact damage taken during compression test. (IM600/#133)

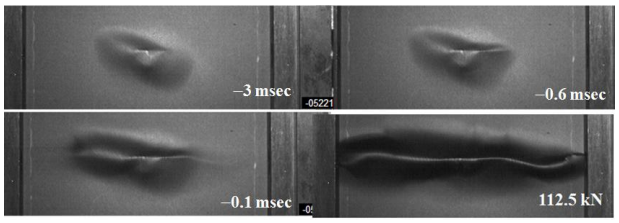

Fig.4 High speed video image of the instant of compression failure. (T700#2500)

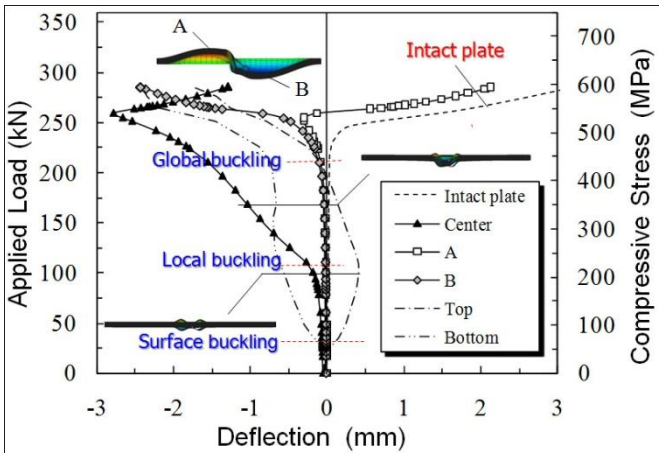

Fig.5 Relationships between applied load and deflection(d_o = 30 mm)

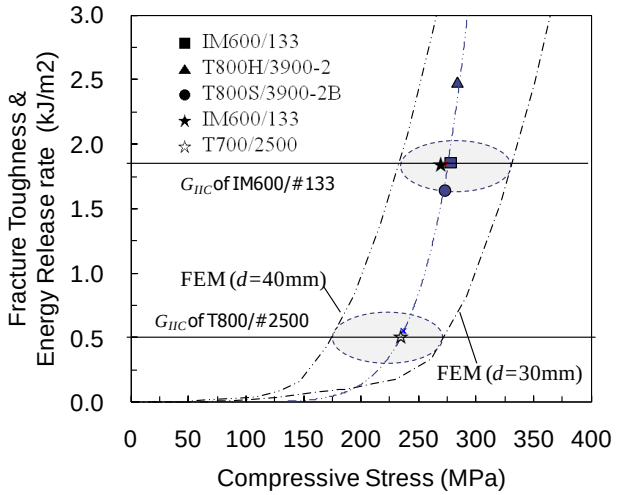

Fig. 6 The relationship between the applied load and maximum energy release rate at the outer edge .(■ ▲ ● : JAXA ACDB database, ★ , ☆ :present experimental results)